

Supplementary information for

**Mechanistic Investigation of cyclohexane oxidation by a binuclear non-heme iron model complex: Evidence of product inhibition by low-temperature stopped-flow studies**

Lauren C. Gregor<sup>†</sup>, Gerard T. Rowe<sup>†</sup>, Elena Rybak-Akimova<sup>‡</sup>, and John P. Caradonna<sup>\*,†</sup>

<sup>†</sup>Department of Chemistry, Boston University, Boston, Massachusetts 02215

<sup>‡</sup>Department of Chemistry, Tufts University, Medford, Massachusetts 02115

Page	Content
S2	<i>Figure S1</i> : 400 MHz <sup>1</sup> H-NMR Spectrum of MPP-OL-Cl <sub>6</sub>
S3	<i>Figure S2</i> : 400 MHz <sup>13</sup> C-NMR Spectrum of MPP-OLCl <sub>6</sub>
S4	<i>Figure S3</i> : 400 MHz <sup>1</sup> H-NMR Spectrum of MPPH-Cl <sub>6</sub>
S5	<i>Figure S4</i> : 400 MHz <sup>13</sup> C-NMR Spectrum of MPPH-Cl <sub>6</sub>
S6	<i>Figure S5</i> : Diode-array spectrum of <b>1</b> with MPPH-Cl <sub>6</sub>
S7	<i>Figure S6</i> : Single-wavelength spectrum of <b>1</b> with MPPH-Cl <sub>6</sub>
S8	<i>Figure S7</i> : Simulation of <i>k<sub>f</sub></i> for MPPH and MPPH-Cl <sub>6</sub>
S9	<i>Figure S8</i> : Heterolytic/homolytic cleavage of MPPH
S10	<i>Figure S9</i> : Time course reactivity of cyclohexane
S11	<i>Figure S10</i> : Effect of single wavelength data by cyclohexanol
S12	<i>Figure S11</i> : Kinetic data and fit for cyclohexanol at 438 nm
S13	<i>Figure S12</i> : Kinetic data and fit for methanol at 438 nm
S14	<i>Figure S13</i> : Kinetic data and fit for MPP-OL at 438 nm
S15	<i>Table S1</i> : Kinetic data for cyclohexanol
S16	<i>Table S2</i> : Kinetic data for methanol
S17	<i>Table S3</i> : Kinetic data for MPP-OL
S18	<i>Figure S14</i> : Electrochemistry of <b>1</b> with cyclohexanol
S19	<i>Figure S15</i> : Inhibition of <b>1</b> utilizing hydroxyurea
S20	Equations used in kinetic fits of model in Scheme 1
S21 – S24	<i>Figures S16-S19</i> : Kinetic data and fit for eliminated models
S25	References

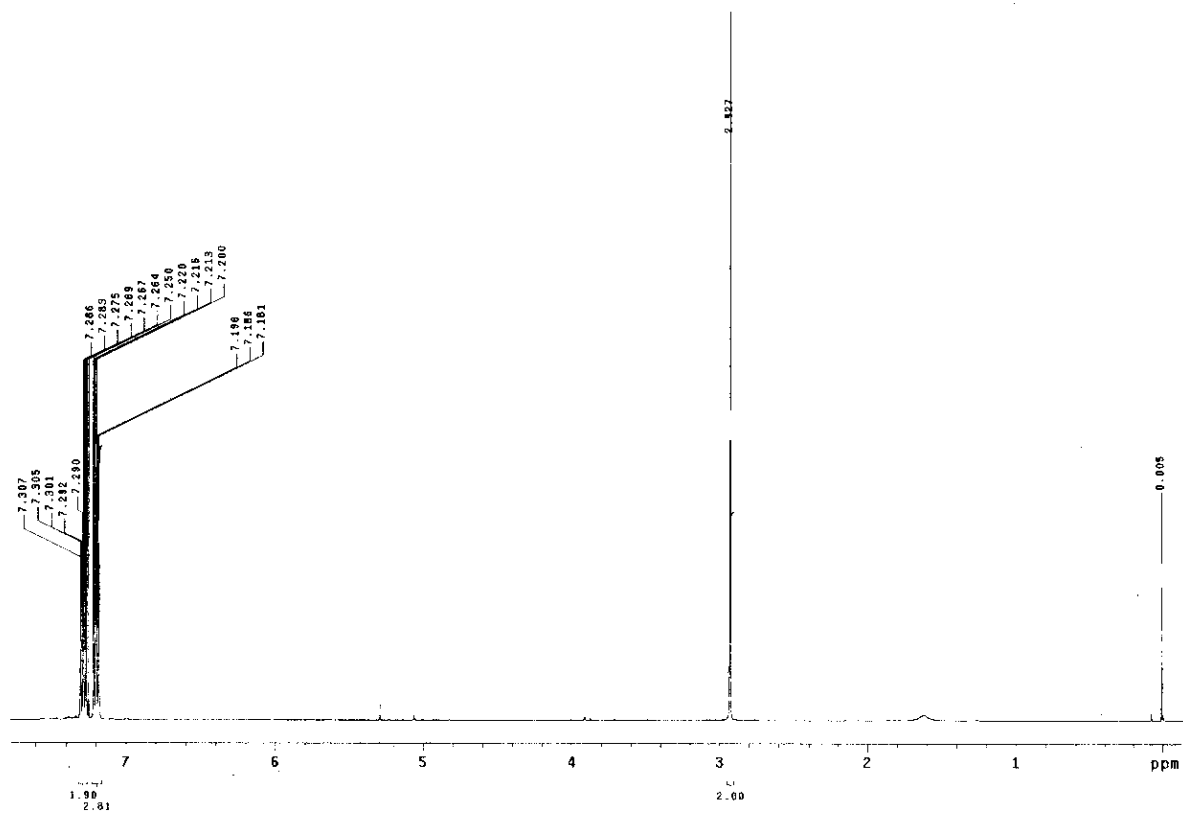


**Figure S1:** 400 MHz <sup>1</sup>H-NMR spectrum of MPP-OL-Cl<sub>6</sub> in CDCl<sub>3</sub>.

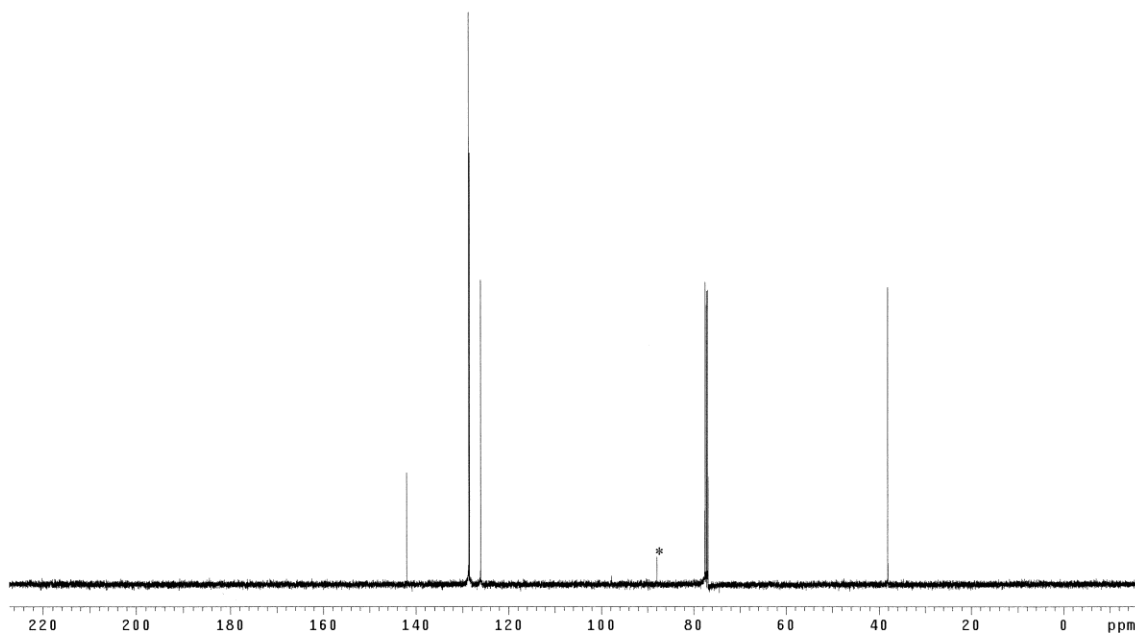


**Figure S2:** 400 MHz  $^{13}\text{C}$ -NMR Spectrum of MPP-OL-Cl<sub>6</sub> in CDCl<sub>3</sub>. Starred peak indicates signal from residual hexachloroacetone starting material.

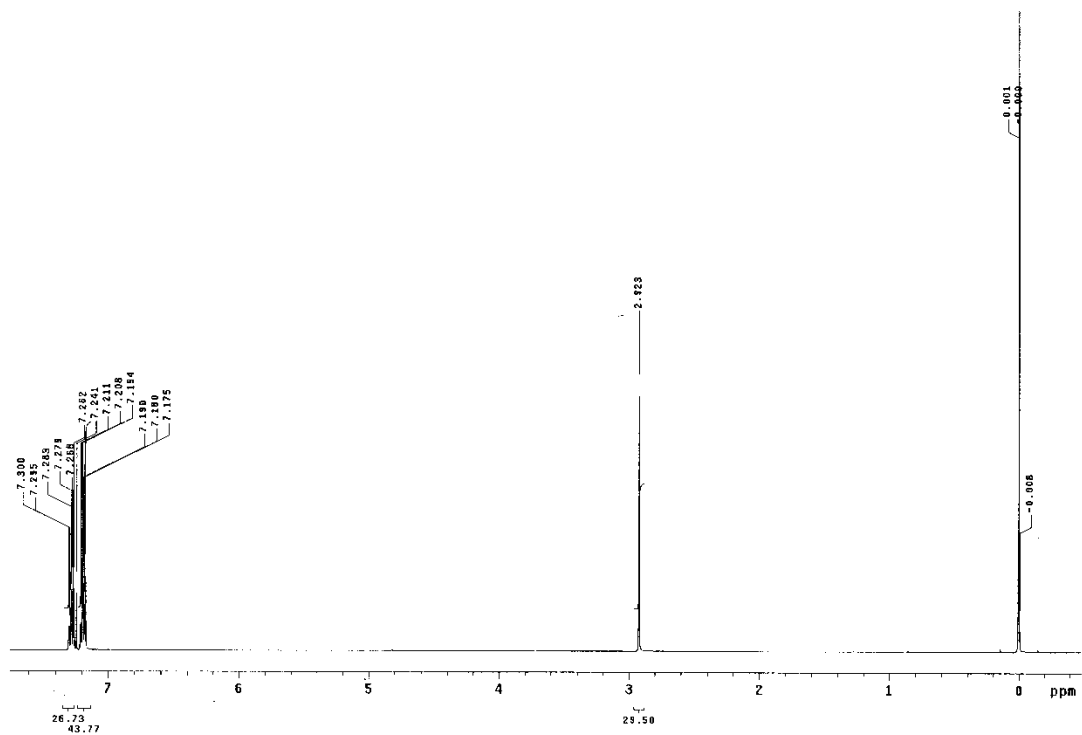


**Figure S3:** 400 MHz <sup>1</sup>H-NMR Spectrum of MPPH-Cl<sub>6</sub> in CDCl<sub>3</sub>.

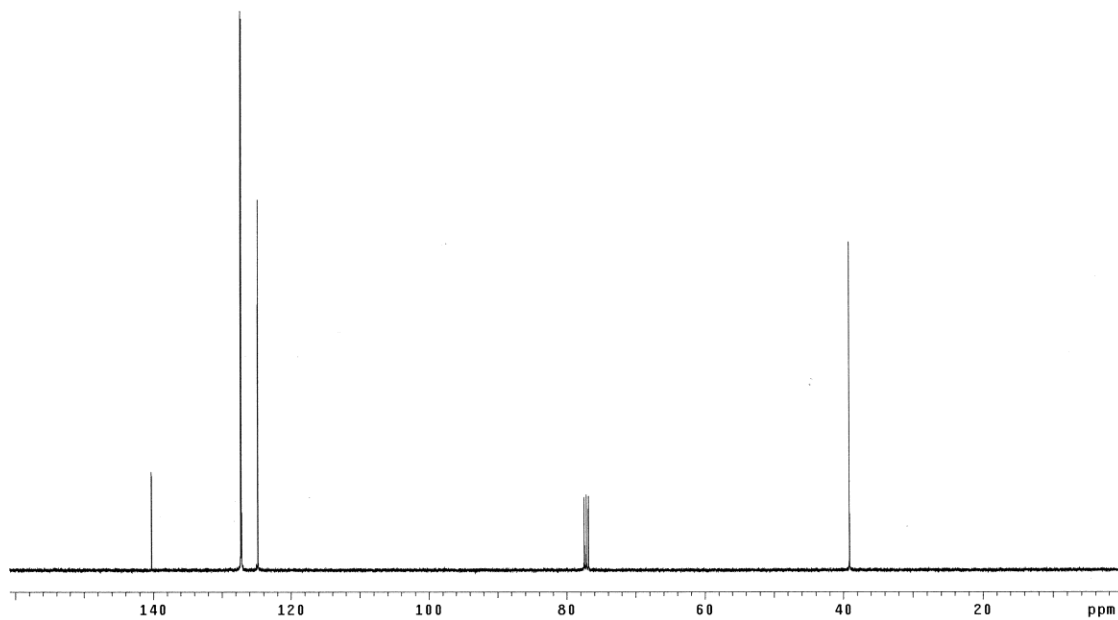


**Figure S4:** 400 MHz  $^{13}\text{C}$ -NMR Spectrum of MPPH- $\text{Cl}_6$  in  $\text{CDCl}_3$ .

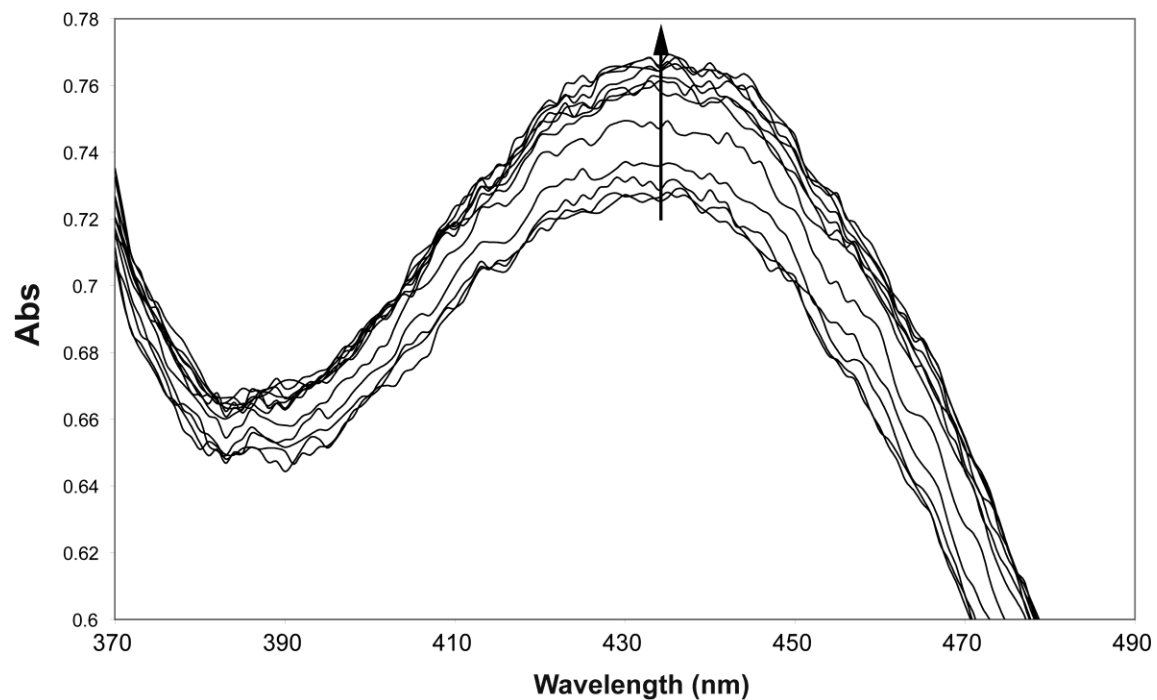


**Figure S5:** Diode-array mode stopped-flow spectra of the reaction of **1** with MPPH-Cl<sub>6</sub> at -75°C. Data represents the first second of the reaction time. [1] = 0.21 mM and [MPPH-Cl<sub>6</sub>] = 53 mM. Scans acquired every 10 ms for a total of 108 samples. 12 scans across the entire time regime displayed here for clarity.

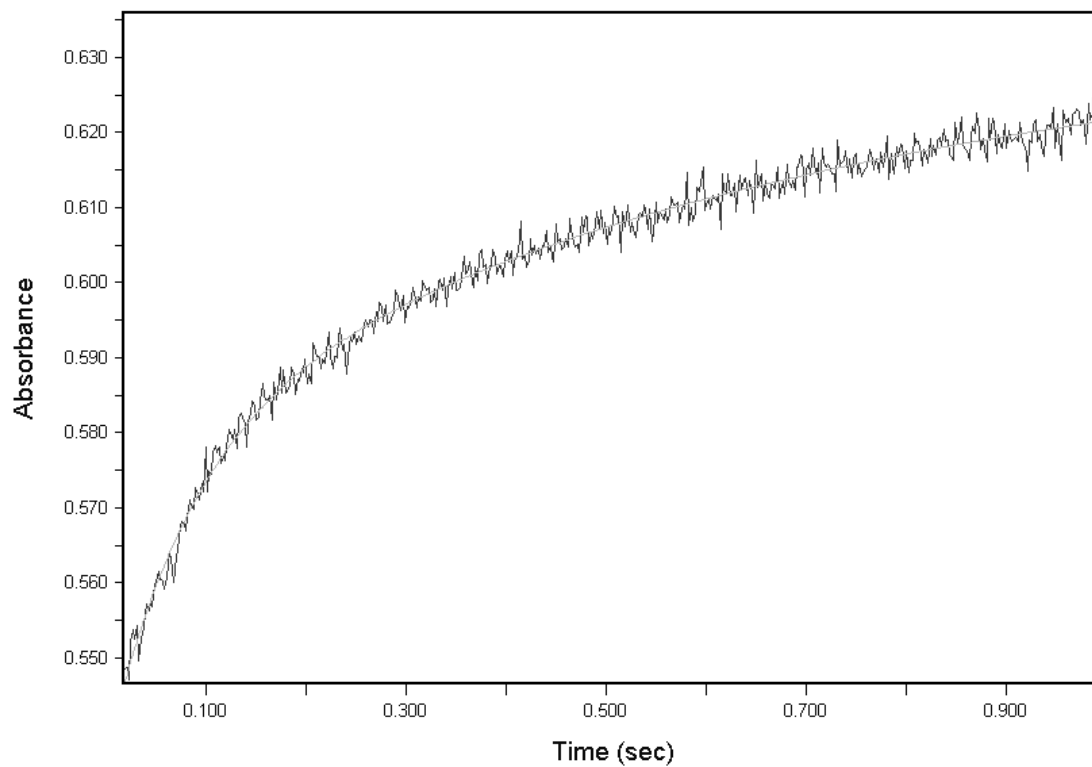


**Figure S6:** Single-wavelength-mode stopped-flow absorbance (438 nm) versus time for the first second of the reaction of MPPH-Cl<sub>6</sub> with **1** at -75°C. [**1**] = 0.21 mM and [MPPH-Cl<sub>6</sub>] = 53 mM.

### Simulation of Intermediate Formation at -75° C

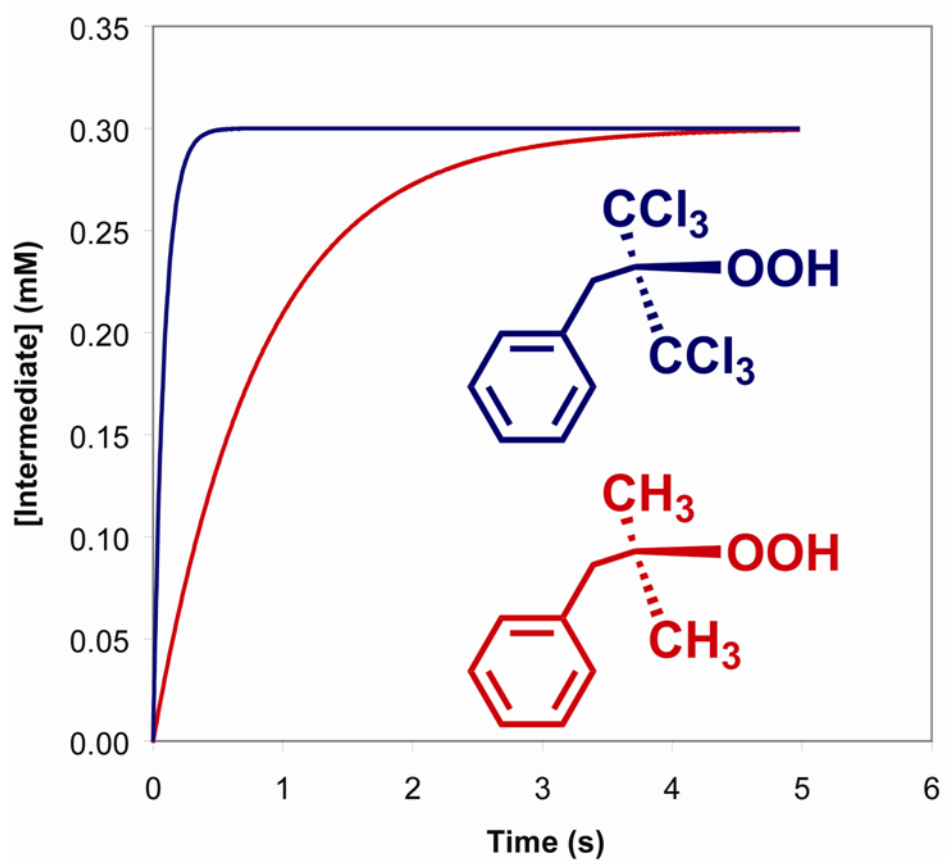


**Figure S7:** Simulation of  $k_1$  reaction using the second order rate constants determined for 1+MPPH and 1+MPPH- $\text{Cl}_6$  reactions measure at -75°C.  $[\mathbf{1}] = 0.3$  mM and  $[\text{R-OOH}] = 50$  mM.



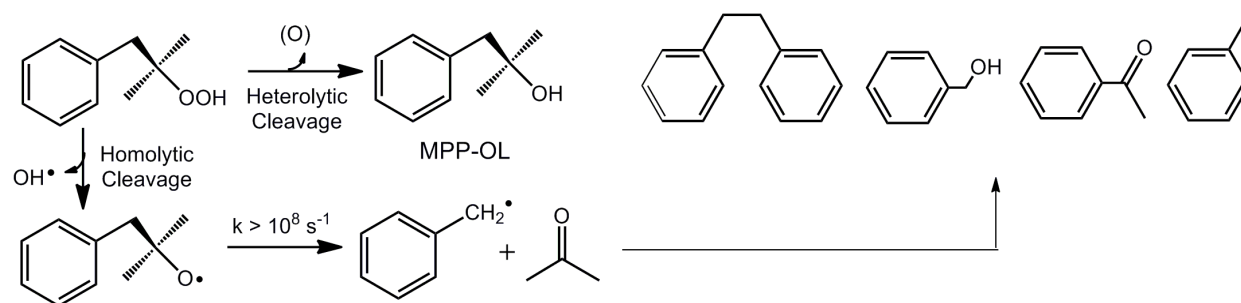


**Figure S8:** Heterolytic/homolytic decomposition pathways of MPPH

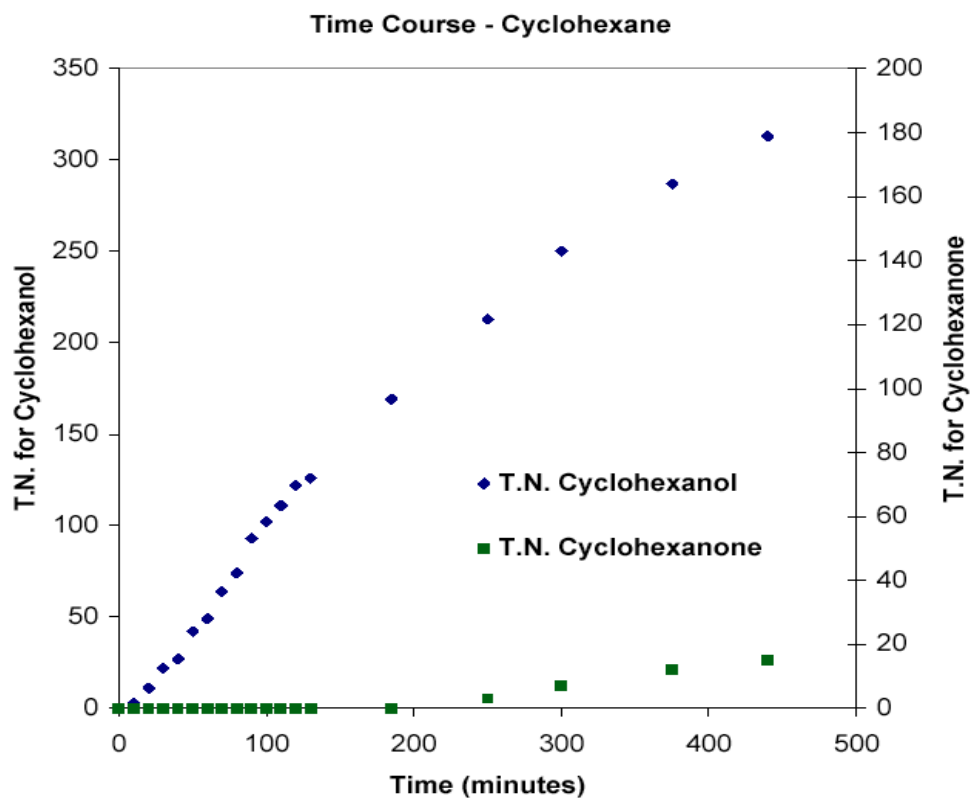


*Figure S9*: Time course reactivity of **1** with MPPH as oxidant and cyclohexane as substrate.

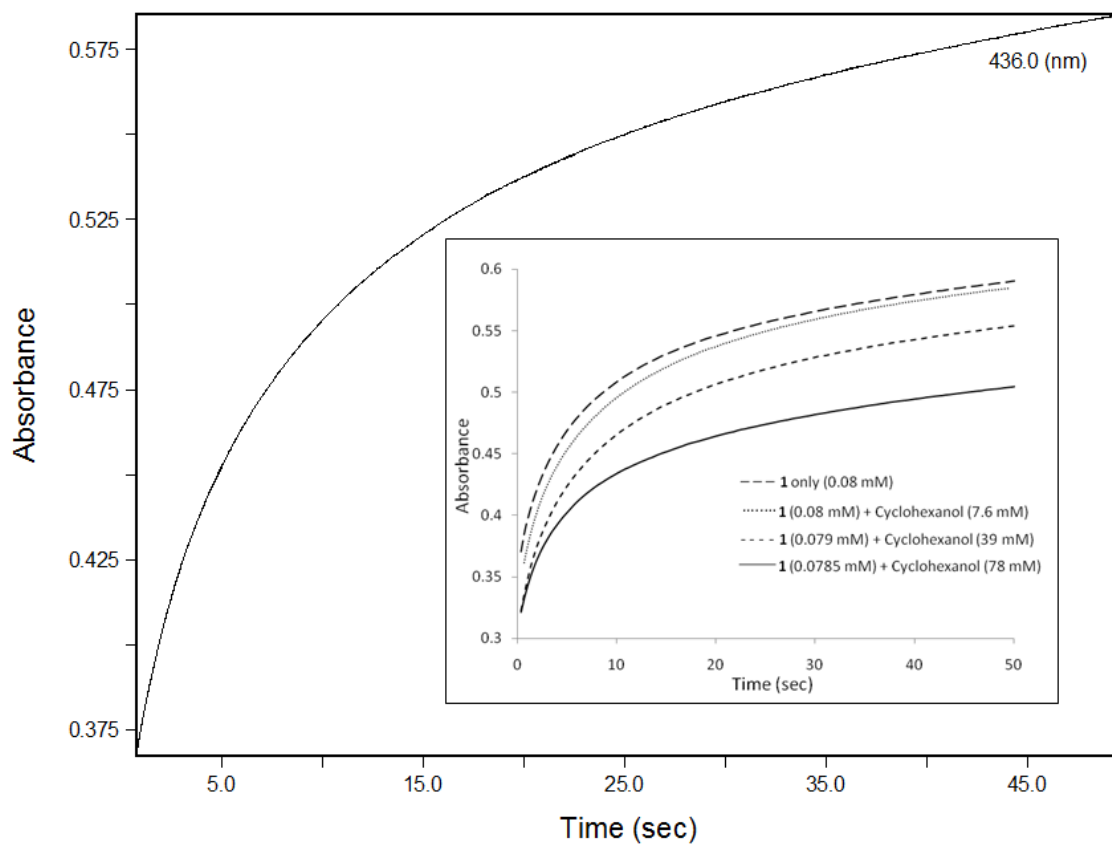


**Figure S10:** Single wavelength data and kinetic fit for **1** (0.08 mM) and MPPH (9.2 mM) with cyclohexanol (7.6 mM). Inset: Effect of single-wavelength data by addition of cyclohexanol

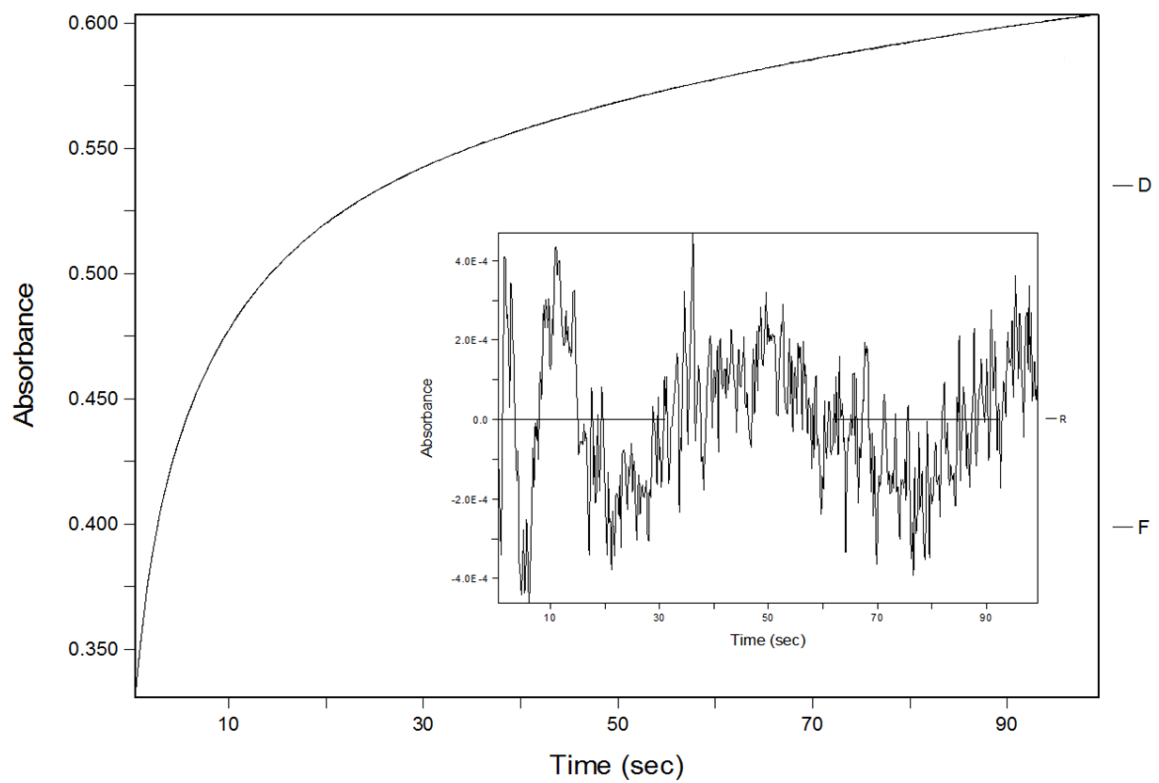


**Figure S11:** Kinetic data at 438 nm and overlay of fit for the reaction of **1** (0.079 mM) and cyclohexanol (78 mM) and 2-methyl-1-phenylprop-2-yl hydroperoxide (9.2 mM) at 193 K. Inset: residuals from fit.

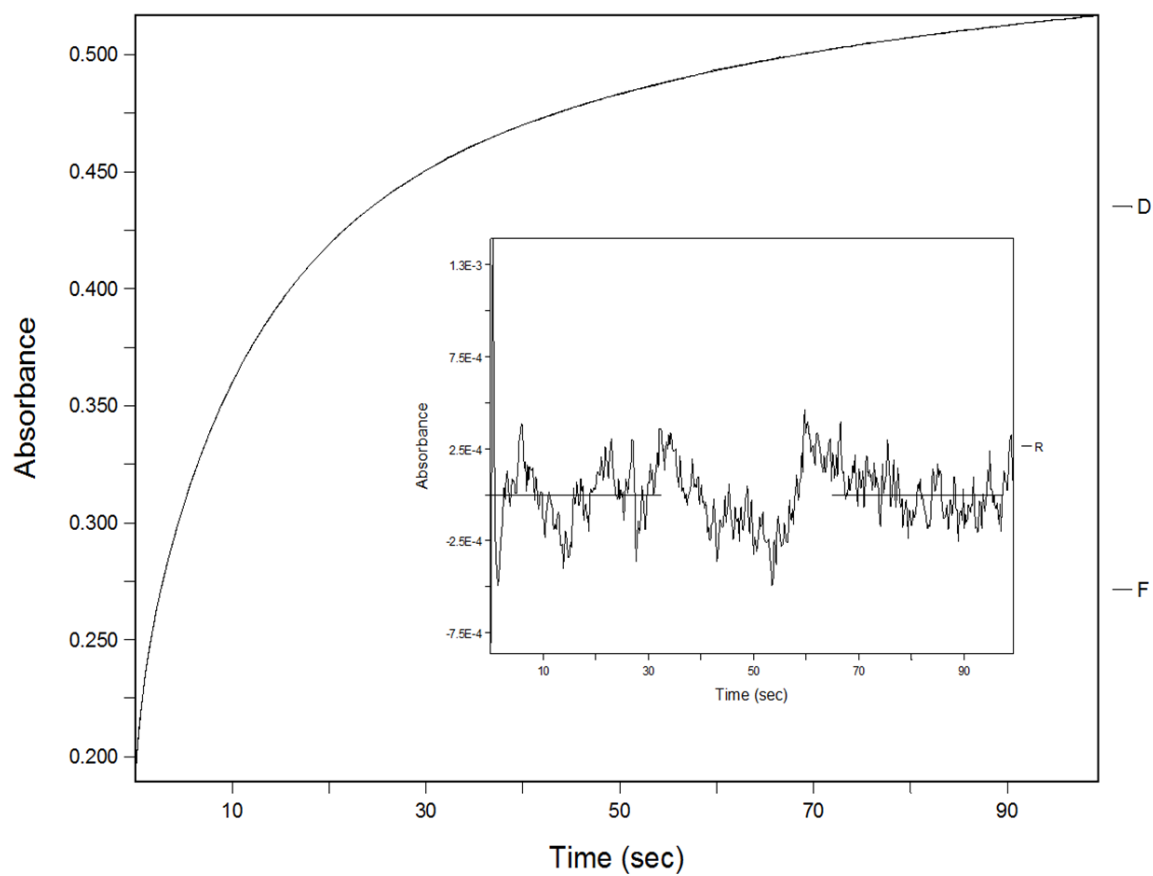


**Figure S12:** Kinetic data at 438 nm and overlay of fit for the reaction of **1** (0.11 mM) and methanol (11 mM) and 2-methyl-1-phenylprop-2-yl hydroperoxide (12.3 mM) at 193 K. Inset: residuals from fit.

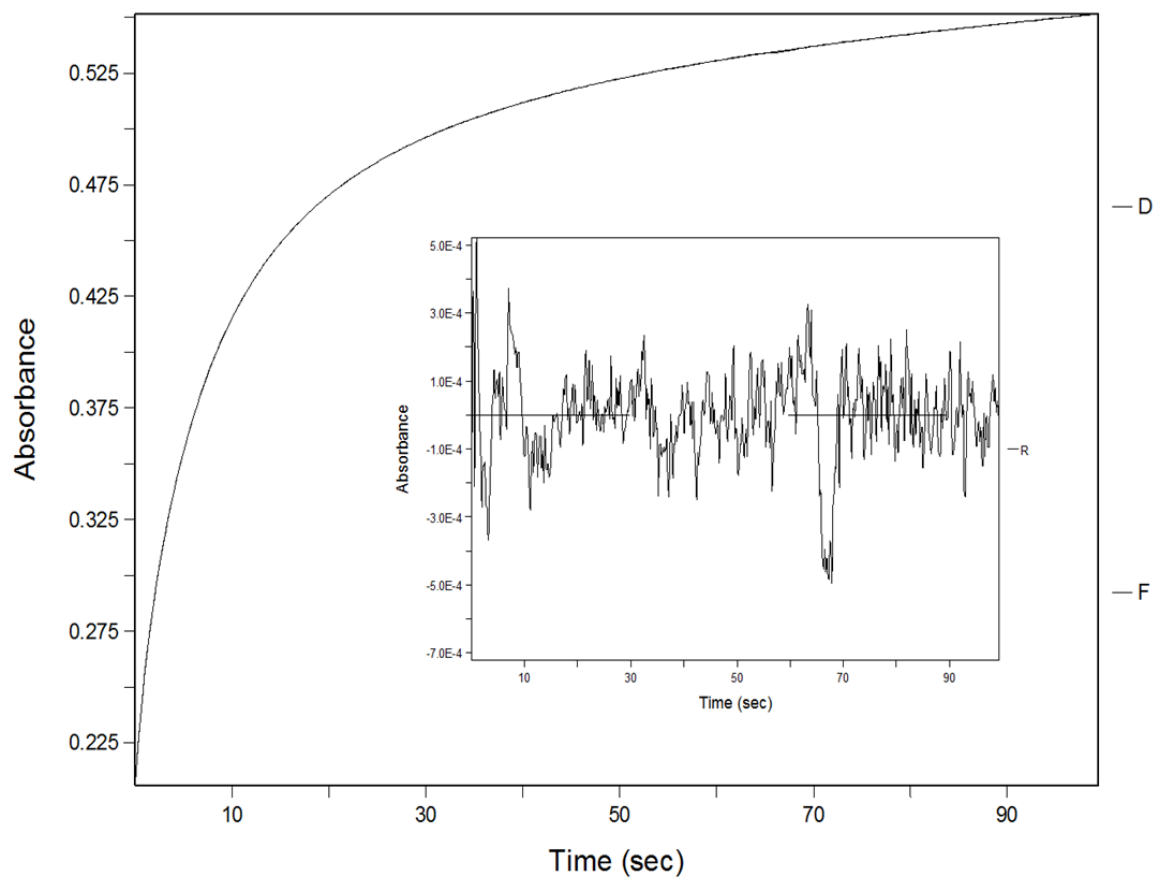


**Figure S13:** Kinetic data and overlay of fit for the reaction of **1** (0.11 mM) and MPP-OL (10.8 mM) and 2-methyl-1-phenylprop-2-yl hydroperoxide (12.1 mM) at 193 K. Inset: residuals from fit.

**Table S1:** Rate data for cyclohexanol

<b>Step</b>	<b>Experiment A</b>	<b>Experiment B</b>	<b>Experiment C</b>	<b>Average</b>
$k_f (\text{M}^{-1}\text{s}^{-1})$	4.326	9.110	4.4894	
$k_r (\text{s}^{-1})$	0.04688	0.04814	0.04578	
$k_1 (\text{s}^{-1})$	0.15 (fixed)	0.15 (fixed)	0.15 (fixed)	
$k_1^{\text{inhib}}_{\text{obs}} (\text{s}^{-1})$	$2.36 \times 10^{-7}$	$3.564 \times 10^{-9}$	$9.93 \times 10^{-9}$	
$k_1^{\text{inhib}} (\text{M}^{-1}\text{s}^{-1})$	$2.65 \times 10^{-5}$	$3.874 \times 10^{-7}$	$1.014 \times 10^{-6}$	
$k_2 (\text{s}^{-1})$	0.1260	0.1167	0.1109	
$k_3 (\text{s}^{-1})$	0.006601	0.004545	0.00634	
<b><math>K_{eq}</math></b>	<b>92.7</b>	<b>189</b>	<b>98.1</b>	<b>127</b>

Experimental conditions:

- A. [1] = 0.08 mM, [cyclohexanol] = 7.6 mM, [MPPH] = 9.2 mM
- B. [1] = 0.079 mM, [cyclohexanol] = 39 mM, [MPPH] = 9.2 mM
- C. [1] = 0.078 mM, [cyclohexanol] = 78 mM, [MPPH] = 9.2 mM

**Table S2:** Rate data for methanol

	<b>Experiment D</b>	<b>Experiment E</b>	<b>Experiment F</b>	<b>Average</b>
$k_f(\text{M}^{-1}\text{s}^{-1})$	7.9634	4.238	0.707	
$k_r(\text{s}^{-1})$	0.0115	0.005659	0.001241	
$k_1(\text{s}^{-1})$	0.15 (fixed)	0.15 (fixed)	0.15 (fixed)	
$k_1^{\text{inhib}}_{\text{obs}}(\text{s}^{-1})$	$1.194 \times 10^{-4}$	$6.994 \times 10^{-5}$	$1.038 \times 10^{-4}$	
$k_1^{\text{inhib}}(\text{M}^{-1}\text{s}^{-1})$	0.009710	0.005868	0.00844	
$k_2(\text{s}^{-1})$	0.1283	0.143	0.1332	
$k_3(\text{s}^{-1})$	0.00536	0.0067	0.00521	
<b><math>K_{eq}</math></b>	<b>692</b>	<b>748</b>	<b>707</b>	<b>716</b>

Experimental Conditions:

D. **[1]** = 0.11 mM,  $[\text{CH}_3\text{OH}]$  = 11 mM,  $[\text{MPPH}]$  = 12.3 mM

E. **[1]** = 0.1095 mM,  $[\text{CH}_3\text{OH}]$  = 54 mM,  $[\text{MPPH}]$  = 12.3 mM

F. **[1]** = 0.109 mM,  $[\text{CH}_3\text{OH}]$  = 109 mM,  $[\text{MPPH}]$  = 12.3 mM



**Table S3:** Rate data for MPP-OL

	<b>Experiment G</b>	<b>Experiment H</b>	<b>Experiment I</b>	<b>Average</b>
$k_f(\text{M}^{-1}\text{s}^{-1})$	8.9281	3.69	2.866	
$k_r(\text{s}^{-1})$	0.0452	0.0144	0.011	
$k_1(\text{s}^{-1})$	0.15 (fixed)	0.15 (fixed)	0.15 (fixed)	
$k_1^{\text{inhib}}_{\text{obs}}(\text{s}^{-1})$	$1.579 \times 10^{-4}$	$4.610 \times 10^{-4}$	$3.398 \times 10^{-4}$	
$k_1^{\text{inhib}}(\text{M}^{-1}\text{s}^{-1})$	0.01305	0.0381	0.02808	
$k_2(\text{s}^{-1})$	0.1156	0.1383	0.1306	
$k_3(\text{s}^{-1})$	0.0062	0.0063	0.003712	
<b><math>K_{eq}</math></b>	<b>197</b>	<b>235</b>	<b>260</b>	<b>230</b>

Experimental Conditions:

G. [1] = 0.11 mM, [MPP-OL] = 10.8 mM, [MPPH] = 12.1 mM

H. [1] = 0.108 mM, [MPP-OL] = 53.5 mM, [MPPH] = 12.1 mM

I. [1] = 0.106 mM, [MPP-OL] = 106 mM, [MPPH] = 12.1 mM

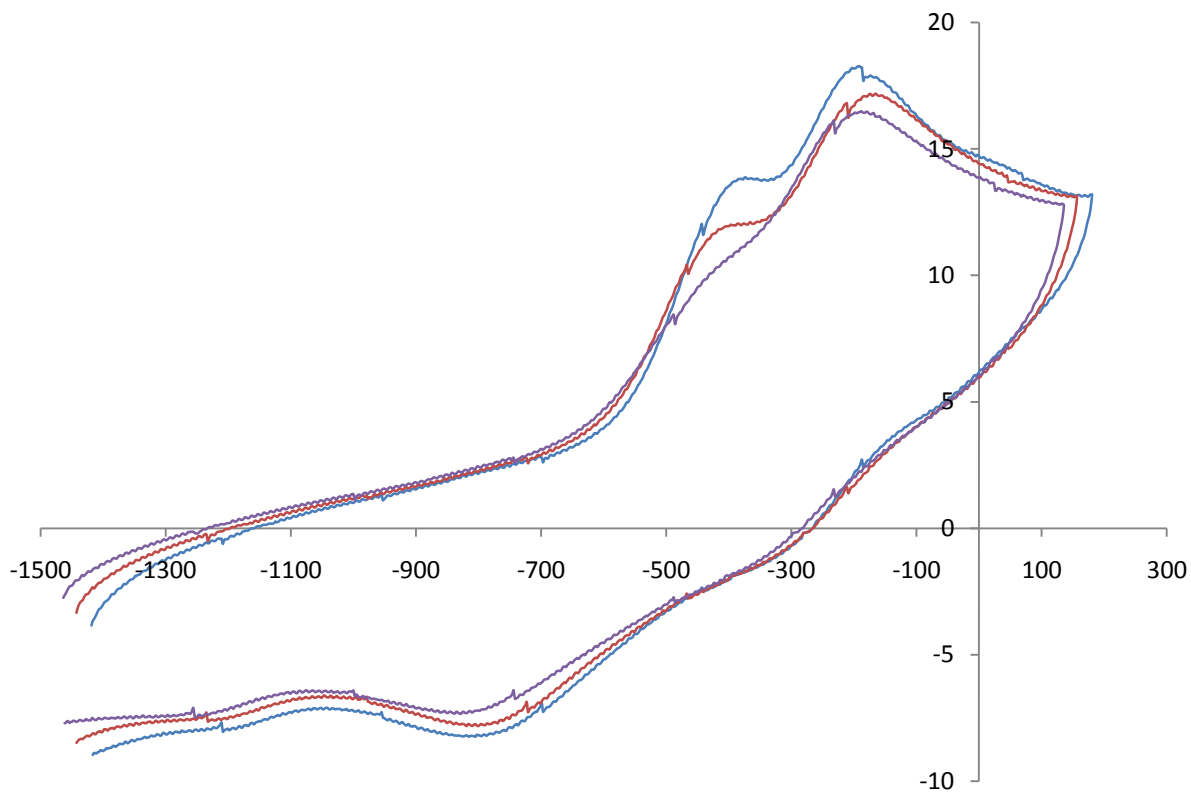


**Figure S14:** Electrochemistry (blue trace) of **1** (0.1 mM) in Electrochemistry (red trace) of **1** (0.098 mM) and cyclohexanol (309 mM). Electrochemistry (purple trace) of **1** (0.091 mM) and cyclohexanol (870 mM). All electrochemistry in DMF with electrolyte (10 mM) and referenced externally to Fc/Fc<sup>+</sup> vs. NHE under anaerobic conditions.

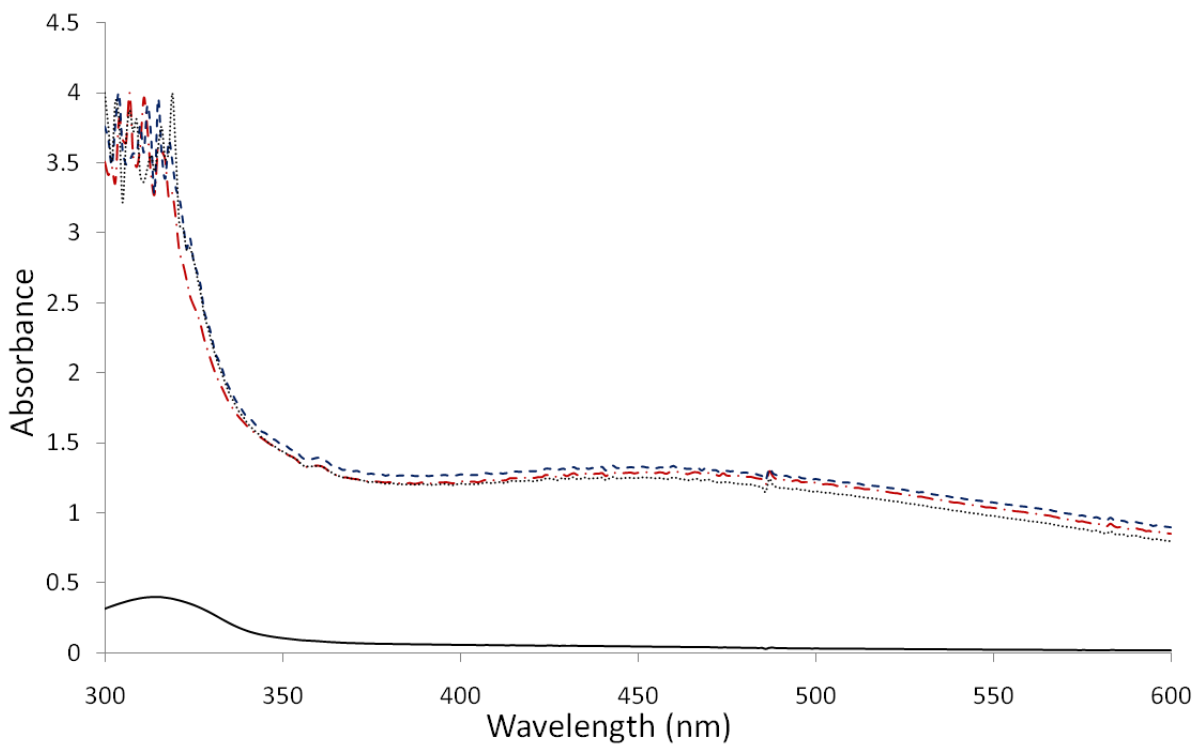


**Figure S15:** UV-vis spectrum of a solution of **1** (0.19 mM) in 70:30 DCM:DMF (v/v) (black line) at  $-74^{\circ}\text{C}$ . A solution of hydroxyurea (0.19 mM) was added to **1** causing a shift in chromophore (red line) followed by the addition of *p*-CN-DMANO (11 mM) (blue line) and no chromophore of **4** observed after 20 minutes (black dashed line)

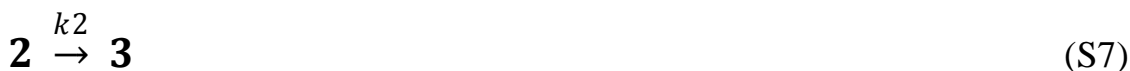
Equations used in kinetic models and fits for the reaction of **1** with MPPH (**X**) in the presence of ROH (S1-S5, S8) and in the absence of substrate (S6, S7, S9-S11, S13):



$$\frac{-d[\mathbf{1}]}{dt} = \frac{d[\mathbf{5}]}{dt} = kf[\mathbf{1}][\text{ROH}] \quad (\text{S3})$$

$$\frac{-d[\mathbf{5}]}{dt} = \frac{d[\mathbf{1}]}{dt} = kr[\mathbf{5}] \quad (\text{S4})$$

$$\frac{-d[\mathbf{5}]}{dt} = \frac{d[\mathbf{6}]}{dt} = k_{1inhib}[\mathbf{5}] \quad (\text{S5})$$



$$\frac{-d[\mathbf{1}]}{dt} = \frac{d[\mathbf{2}]}{dt} = k_1[\mathbf{1}][\text{MPPH}] \quad (\text{S10})$$

$$\frac{-d[\mathbf{2}]}{dt} = \frac{d[\mathbf{3}]}{dt} = k_2[\mathbf{2}] \quad (\text{S11})$$

$$\frac{-d[\mathbf{6}]}{dt} = \frac{d[\mathbf{3}]}{dt} = k_2[\mathbf{6}] \quad (\text{S12})$$

$$\frac{-d[\mathbf{3}]}{dt} = \frac{d[\mathbf{4}]}{dt} = k_3[\mathbf{3}] \quad (\text{S13})$$

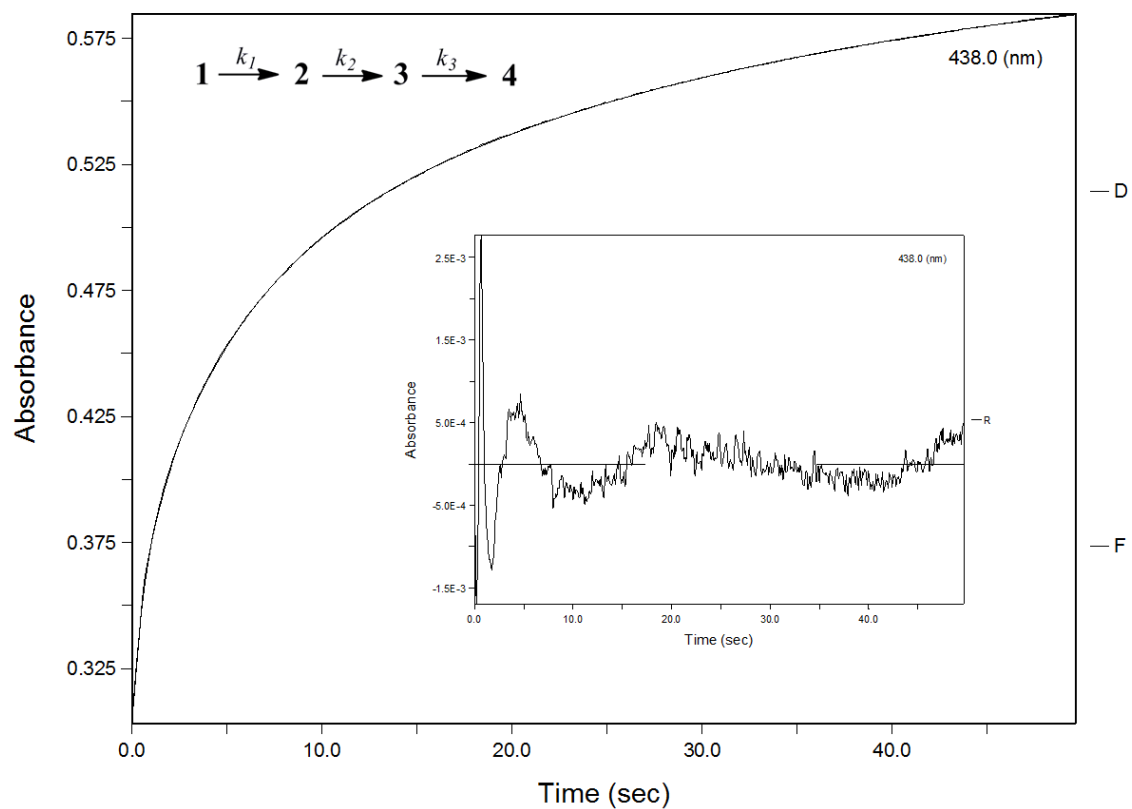


**Figure S16:** Kinetic fit and residuals (Inset) for models that did not result in adequate fits to the data.

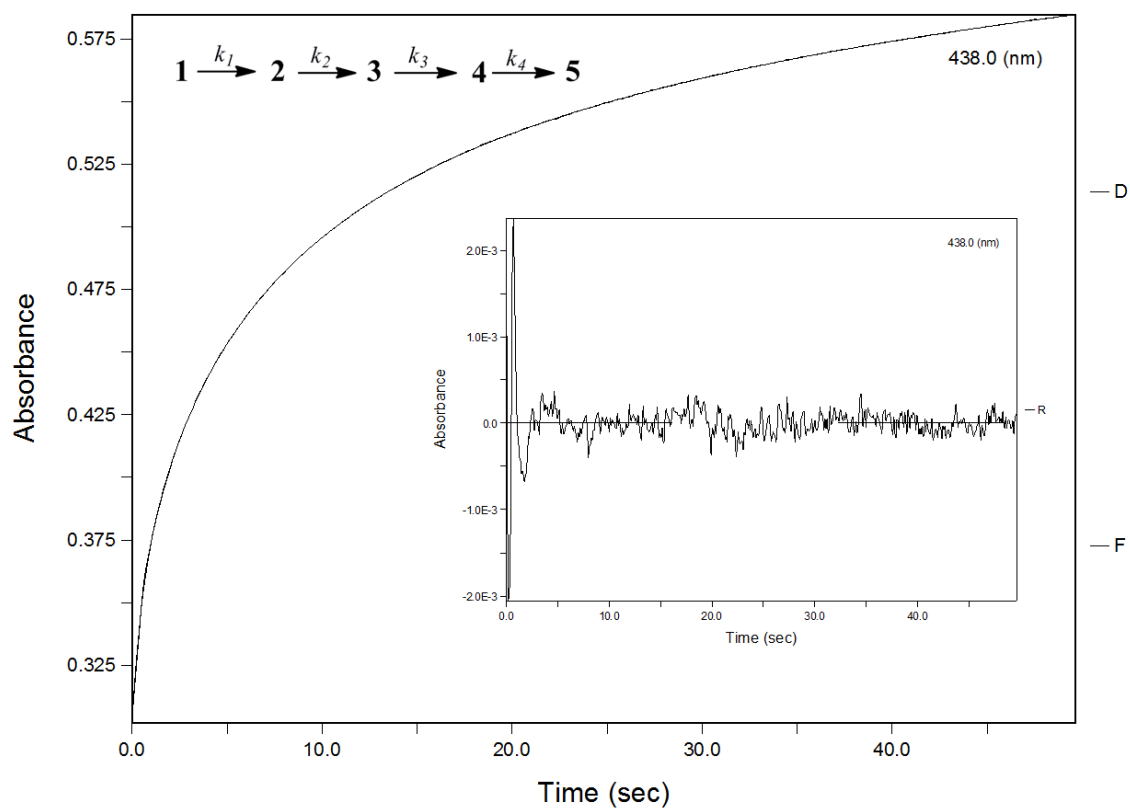


**Figure S17:** Kinetic fit and residuals (Inset) for models that did not result in adequate fits to the data.



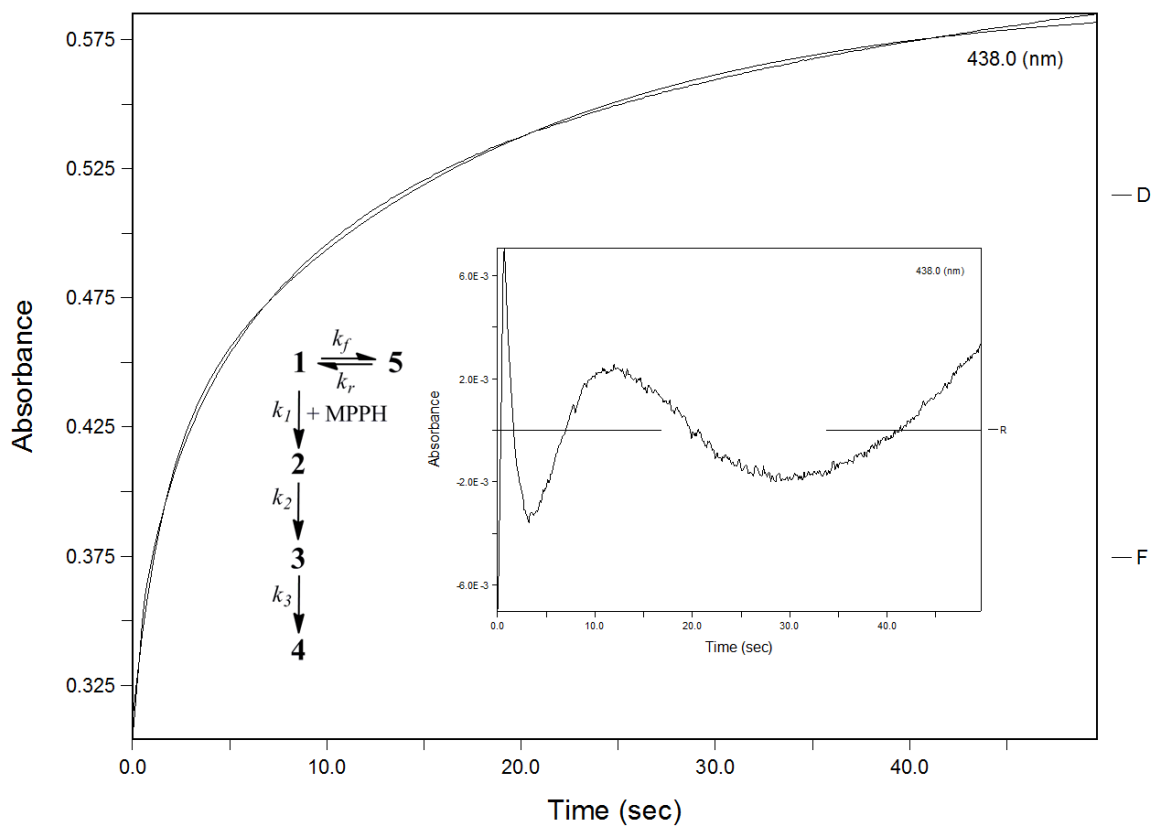


**Figure S19:** Kinetic fit and residuals (Inset) for models that did not result in adequate fits to the data.



**References:**

- S1. S. Mukerjee, A. Stassinopoulos and J. P. Caradonna, *Journal of the American Chemical Society*, 1997, **119**, 8097-8098.
- S2. T. L. Foster and J. P. Caradonna, *Journal of the American Chemical Society*, 2003, **125**, 3678-3679.
- S3. R. R. Hiatt and W. M. J. Strachan, *Journal of Organic Chemistry*, 1963, **28**, 1893-1894.
- S4. G. T. Rowe, C. E. Rogge, E. V. Rybak-Akimova and J. P. Caradonna, *Chemistry--A European Journal*, 2008, **14**, 8303-8311.
- S5. D. A. Skoog, D. M. West, and F. J. Holler. *Fundamentals of Analytical CHEMistry*; 7<sup>th</sup> ed.; Harcourt Brace & Company: Orlando, 1996.